

Dual-Band Dual Circular Polarization Filter Antenna Based on Transmission Line Feed

Wei Luo*, Wuquan Chen, and Yi Ren

Abstract—The uplink and downlink of modern satellite communication systems operate on different frequency bands. A novel dual-band dual circular polarization filter antenna with a single port is proposed in this paper. The dual-band characteristic of the antenna is obtained by exciting stacked patches. The antenna supports right-handed circular polarization (RHCP) at lower frequency band and left-handed circular polarization (LHCP) at higher frequency band, respectively. The feeding network is realized with a strip line, and the antenna can be equivalent to a parallel circuit. If the lower frequency patch works, the higher frequency patch presents high impedance, and vice versa. Therefore, the antenna has excellent filtering performance. The measurements of antenna prototype are in good agreement with the simulation results. The impedance bandwidth is 5.80–6.10 GHz and 9.20–10.64 GHz, and the axial ratio (AR) bandwidth is 40 MHz for lower band and 180 MHz for higher band, respectively. Meanwhile, the radiation pattern is stable in the operation frequency bands.

1. INTRODUCTION

Generally, uplink and downlink of modern satellite communication systems operate on different frequencies [1, 2]. If a dual-band dual circular polarization antenna with shared aperture is used, the size and cost of the system could be greatly reduced [3]. In the application of satellite communication [4–6], a circular polarization antenna [7, 8] receives the incoming wave of arbitrary linear polarization, of which radiated electromagnetic wave could also be received by any linear polarization antenna. Therefore, the relative installation attitudes of the transmitting and receiving antennas are not limited by the torsion angle for the circular polarization antenna. In a vehicle satellite communication system, accurate alignment of the receiver in the vehicle will be extremely difficult for linear polarization, but not for circular polarization [9, 10]. The dual-band dual circularly polarized antenna achieves different circular polarization characteristics (right-handed circular polarization (RHCP) or left-handed circular polarization (LHCP)) at lower and higher frequency bands. Therefore, the research of dual-band dual circular polarization antenna with shared aperture fed by single port has significant engineering application value for vehicle satellite communication system.

At present, many approaches have been applied to design dual-band dual circularly polarized antennas. In [11] and [12], a long strip coupling feeding structure and a circular arc coupling feeding structure are used to feed two microstrip metal patches at the same time, respectively. However, these two methods adopt coaxial feeding method, which are very difficult to be applied to large antenna array and are not suitable for communication systems requiring high gain. Another important method to realize dual-band dual circular polarizations is the sequential rotation technique [13]. This method requires two different feed networks and four identical antenna units, which increases the design difficulty and processing costs.

Received 14 January 2022, Accepted 8 April 2022, Scheduled 17 April 2022

* Corresponding author: Wei Luo (luoweil@cqupt.edu.cn).

The authors are with the College of Photoelectric Engineering, Chongqing University of Posts and Telecommunications, Chongqing 400065, China.

A shared aperture dual-band dual circular polarization filter antenna fed by a single port is proposed in this paper. Two patches of different frequency bands share the same dielectric substrate. The antenna has good impedance matching at 5.80–6.10 GHz and 9.20–10.64 GHz, supporting RHCP and LHCP, respectively. One transmission line with branch is used to feed two patches. By optimizing the length of transmission line, higher and lower frequency patches can work independently at the same time.

2. ANTENNA CONFIGURATION

The antenna consists of two patches as radiators, which share the same dielectric substrate. The higher frequency patch is placed on the upper layer, and the lower frequency patch is placed on the lower layer. Fig. 1 shows the geometry of a dual-band dual circularly polarized stacked microstrip antenna fed by a single port. To feed the higher frequency patch, a square slot is etched in the center of the lower frequency patch, resulting in a narrow bandwidth for the lower band. Two vertical slots are cut on the ground to feed the two patches, respectively. The patches are etched on an FR4 substrate with a thickness of 0.508 mm. The relative dielectric constant of the substrate is 4.4, and the loss tangent is 0.02. There is an air layer between the two substrates. By optimizing the thickness of the air layer, a good coupling strength between the gaps and the radiators is realized. The feeding network with the filtering function is etched at the bottom of the lower dielectric substrate. The length of higher frequency feeding line is larger than that of the lower frequency feeding line. The design is optimized by HFSS, and the optimized structural parameters are shown in Table 1.

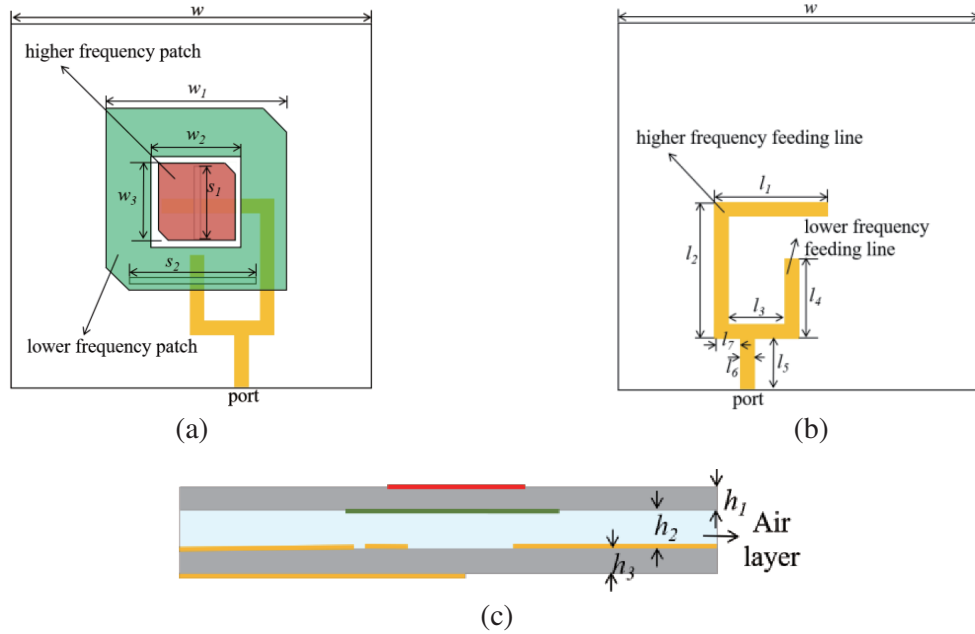


Figure 1. Geometry of the proposed antenna. (a) Top view. (b) Bottom view. (c) Side view.

Table 1. The antenna parameters (mm).

| w | w_1 | w_2 | w_3 | s_1 | s_2 | h_1 | h_2 |
|-------|-------|-------|-------|-------|-------|-------|-------|
| 50.0 | 15.0 | 8.0 | 7.2 | 7.2 | 10.2 | 0.508 | 1.0 |
| h_3 | l_1 | l_2 | l_3 | l_4 | l_5 | l_6 | l_7 |
| 0.508 | 9.8 | 12.3 | 4.3 | 8.3 | 13.2 | 1.0 | 2.0 |

3. ANTENNA PRINCIPLE ANALYSIS

Two patches operating in different frequency bands are fed through the same port. The antenna consists of two patches as radiation elements, which can be equivalent to the parallel circuits, as shown in Fig. 2, where G and B are conductance and susceptance, respectively. In general, these two patches may affect each other. However, the feeding network has filtering characteristics, and the mutual coupling between higher and lower frequency patches can be reduced only by optimizing the length of the feeding lines. If the antenna is fed in the lower frequency band, the higher frequency patch does not radiate electromagnetic wave, which is only used as a passive patch. Under this condition, the higher frequency feeding strip line is regarded as an open-stub. The length of the open-stub is within $1/4$ wavelength, and the impedance theoretically changes from 0 to infinity. Therefore, high impedance can be achieved by adjusting the length of higher frequency feeding strip line. Similarly, when the antenna operates in the higher frequency band, tuning the length of the lower frequency feeding strip line can also achieve high impedance. As shown in Fig. 3, when the lower frequency patch is excited, the higher frequency feeding strip line is used as the lower frequency filter branch, and vice versa.

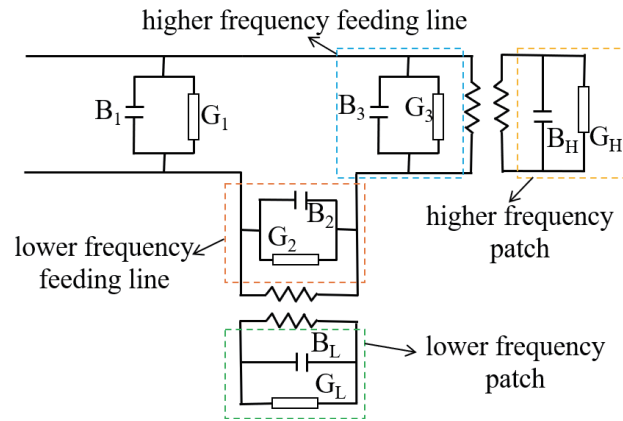


Figure 2. Transmission line equivalent circuit of the antenna.

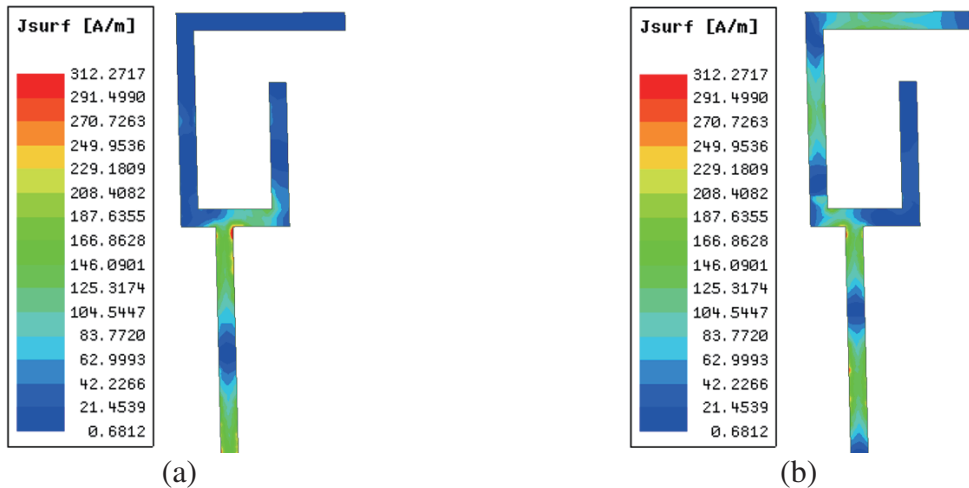


Figure 3. The surface current distribution of the feeding network. (a) 5.93 GHz. (b) 9.60 GHz.

The filtering performance of the feeding network is discussed, as shown in Fig. 4. Since the feeding network with filtering performance is introduced into the antenna design, the antenna has filtering performance. The integrated design of antenna and filter is realized. By optimizing the size of antenna and feeding network, good impedance matching of antenna port can be realized.

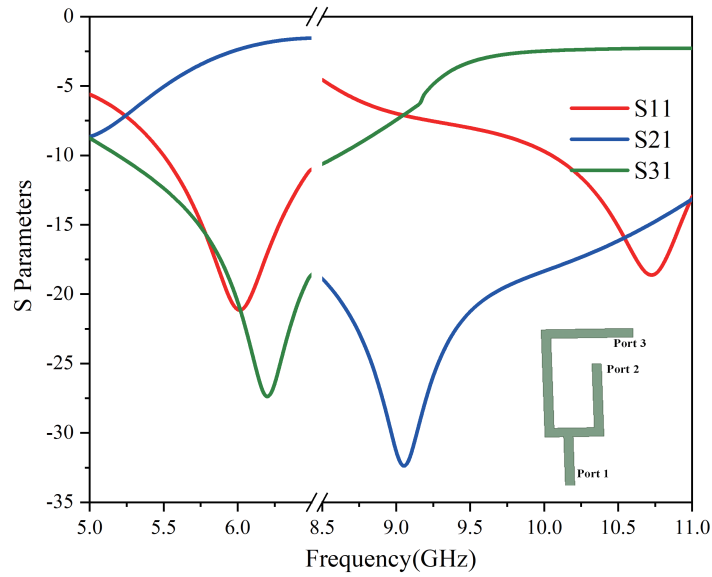


Figure 4. Simulation S parameters of feeding network.

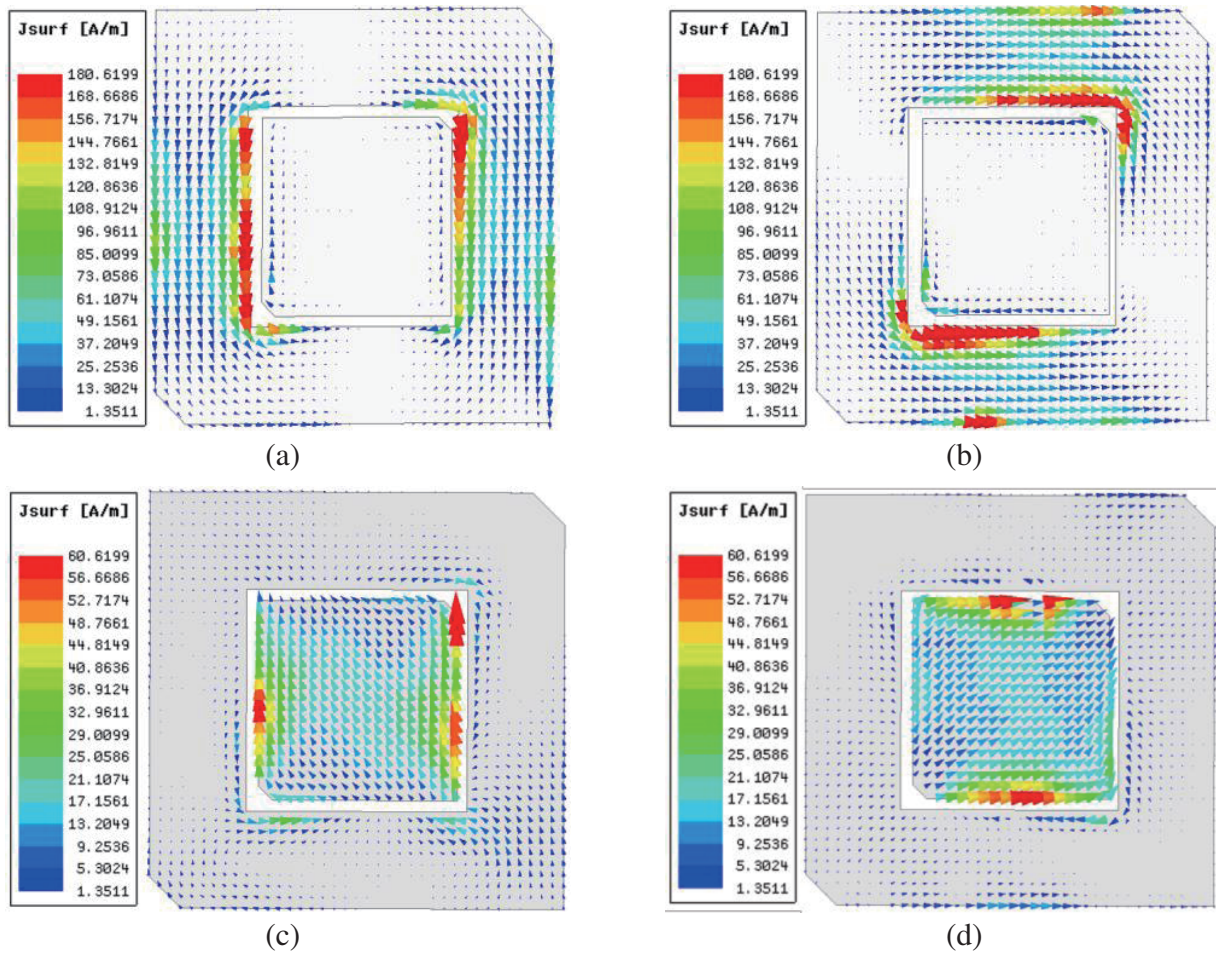


Figure 5. The surface current distribution of the antenna. (a) $t = 0$ at 5.93 GHz. (b) $t = T/4$ at 5.93 GHz (T is the period). (c) $t = 0$ at 9.60 GHz. (d) $t = T/4$ at 9.60 GHz.

The surface current distributions of the patches at different times of different frequencies are shown in Fig. 5. The electric current is mainly distributed on the surface of lower frequency patch at 5.93 GHz, and there is weak current at the edge of higher frequency patch due to coupling, as shown in Figs. 5(a), (b). The current is mainly distributed on the surface of higher frequency patch at 9.60 GHz, and lower frequency patch is only used as parasitic patch, as shown in Figs. 5(c), (d). Therefore, higher and lower frequency patches are isolated because they work in two different frequency bands without overlap. This isolation ensures that each patch can be designed separately. It can be seen that the two patches work independently. While the surface current of the antenna rotates counterclockwise to achieve RHCP at 5.93 GHz in lower frequency band, LHCP is generated by the clockwise rotated surface current at 9.60 GHz in higher frequency band.

4. SIMULATED AND MEASURED RESULTS

In order to verify the reliability of the simulation results, the antenna is processed and measured, as shown in Fig. 6. Fig. 7 shows the S parameters of the proposed dual-band dual circular polarization antenna. The lower frequency band of the antenna is 5.80–6.10 GHz, and the higher frequency band is 9.20–10.64 GHz. In these two bands, the antenna shows frequency selectivity and good impedance matching. As shown in Fig. 8, the lower frequency axial ratio (AR) bandwidth of the antenna is 40 MHz, and the measured higher frequency bandwidth of $AR < 3$ dB is 9.55–9.73 GHz. The gain of the antenna is greater than 6.7 dBic in the operating bands. The gain of the antenna is relatively stable in the working frequency bands, and the out-of-band gain of lower frequency quickly drops to -9 dBic, showing good filtering characteristics. The radiation efficiency of the proposed antenna is shown in Fig. 9. The radiation efficiency in the lower frequency band is higher than 80% in the range of 5.82–6.08 GHz, which drops rapidly to 35% out-of-band to indicate that the antenna has good filtering performance. The radiation efficiency of the higher frequency band is very stable, which is higher than 80%.

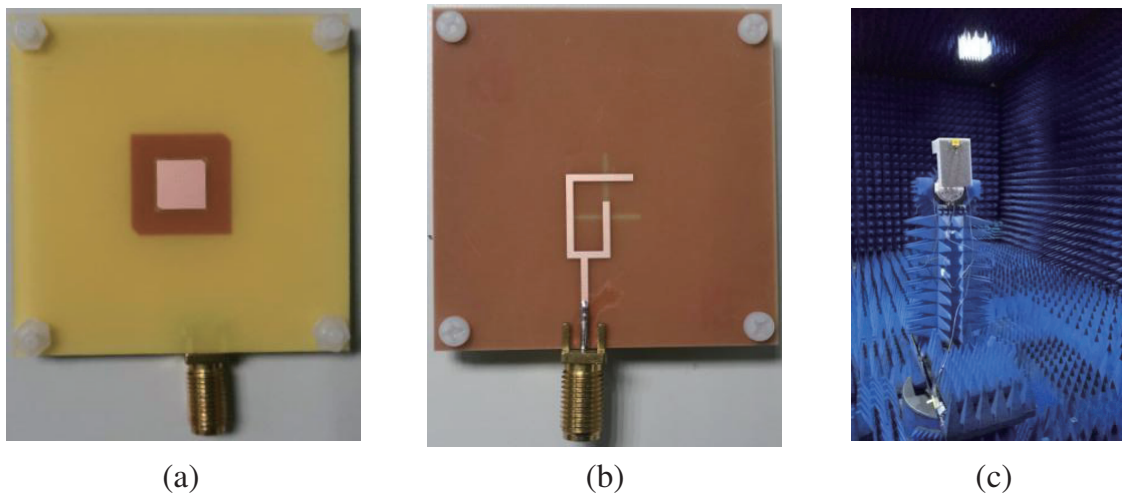


Figure 6. Prototype of the antenna. (a) Top view. (b) Bottom view. (c) Test scenario.

The measured radiation patterns are in good agreement with the simulations, as shown in Fig. 10. At the same time, the measured cross polarization is greater than 18 dB for lower frequency and greater than 25 dB for higher frequency band, respectively. In the backward direction, the cross-polarization gain is significantly higher than the co-polarization gain, which is caused by the radiation of the feeding network.

The designed antenna is compared with the existing works, as shown in Table 2. The comparison involves the number of feeding ports, filtering characteristics, impedance bandwidth, AR bandwidth,

and peak gain of the antenna. It can be seen from the comparison that the designed antenna has a wide impedance bandwidth and stable radiation pattern. In addition, the proposed antenna also has filtering characteristics, which can achieve isolation between transmitting and receiving channels.

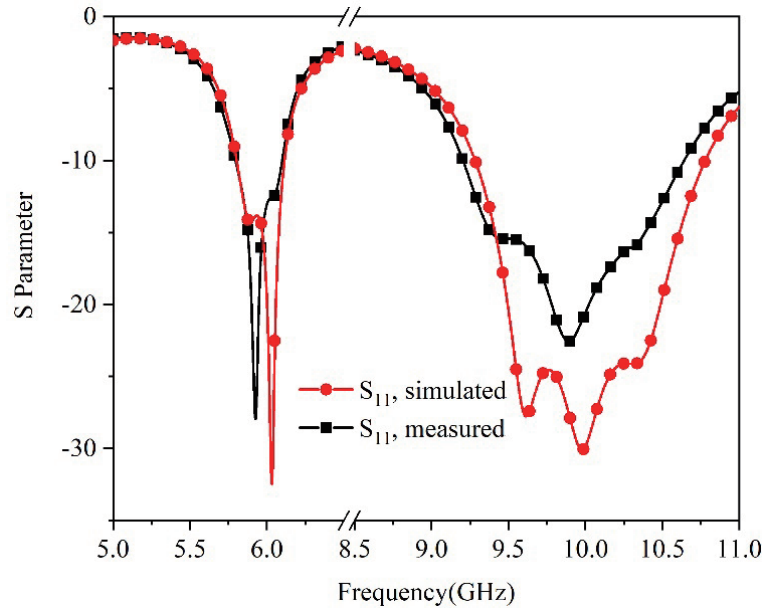


Figure 7. S parameters of the antenna.

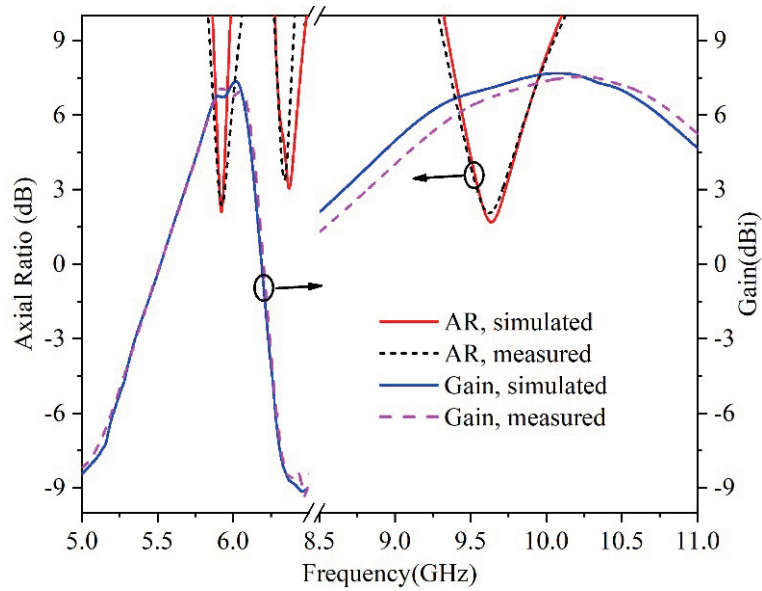


Figure 8. AR and gain of the antenna.

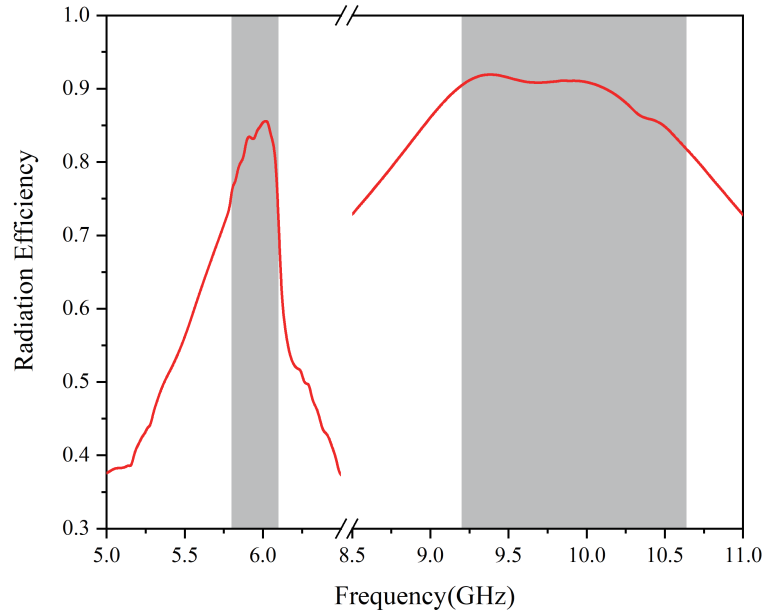


Figure 9. Efficiency of the proposed antenna.

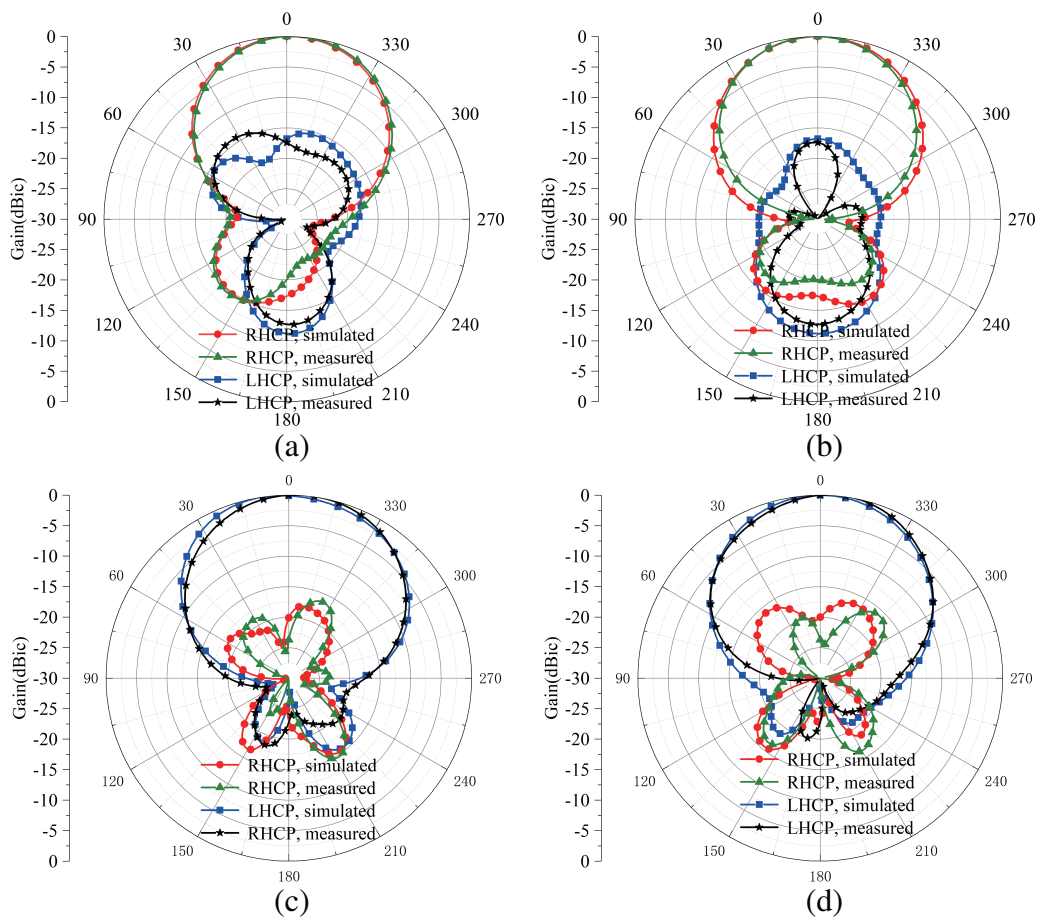


Figure 10. Radiation pattern of antenna at different frequencies. (a) $\Phi = 0^\circ$ at 5.93 GHz. (b) $\Phi = 90^\circ$ at 5.93 GHz. (c) $\Phi = 0^\circ$ at 9.66 GHz. (d) $\Phi = 90^\circ$ at 9.66 GHz.

Table 2. Comparison of different dual-band dual circular polarization antennas.

| References | Ports | Filtering feature | Bandwidth (GHz) | AR band (MHz) | Gain (dBic) |
|------------|--------|-------------------|-----------------------------|---------------|---------------------|
| [1] | Single | yes | 11.68–12.50, 17.20–18.40 | 200, 350 | 18, 18.2 (array) |
| [2] | Single | no | 2.48–2.57, 2.57–3.69 | 18, 22 | 10.8, 12.5 |
| [3] | Single | no | 8.32–9.83 | 110, 140 | 5.8, 4 |
| [12] | Single | no | 2.08–2.12, 3.55–3.65 | 9, 21 | 8.4, 9.9 |
| This work | Single | yes | 5.80–6.10, 9.20–9.64 | 40, 180 | 6.7, 7.2 |

5. CONCLUSION

In this paper, a filter antenna based on transmission line feeding is designed, which supports dual-band dual circular polarization operation. The antenna is composed of a square patch and a ring patch, which can be regarded as a parallel circuit. The filtering characteristic is obtained by adjusting the length of higher and lower frequency feeding branch lines, and the mutual coupling of the two patches is reduced. In the operating frequency bands, the antenna has good impedance matching and flat gain. The designed antenna can be used as a promising candidate for satellite communication system.

ACKNOWLEDGMENT

This work was supported by the Science and Technology Research Program of Chongqing Municipal Education Commission under Grant (number KJQN202000623); and National Natural Science Foundation of China under Grant (number 61871063).

REFERENCES

1. Zhang, J., W. Wu, and D. Fang, "Dual-band and dual-circularly polarized shared-aperture array antennas with single-layer substrate," *IEEE Transactions on Antennas and Propagation*, Vol. 64, 109–116, 2016.
2. Zhang, J., L. Zhu, N. Liu, and W. Wu, "Dual-band and dual-circularly polarized single-layer microstrip array based on multiresonant modes," *IEEE Transactions on Antennas and Propagation*, Vol. 65, 1428–1433, 2017.
3. Kumar, K., S. Dwari, and M. K. Mandal, "Dual-band dual-sense circularly polarized substrate integrated waveguide antenna," *IEEE Antennas and Wireless Propagation Letters*, Vol. 17, 521–524, 2018.
4. Wang, S., L. Zhu, G. Zhang, J. Yang, J. Wang, and W. Wu, "Dual-band dual-CP all-metal antenna with large signal coverage and high isolation over two bands for vehicular communications," *IEEE Transactions on Vehicular Technology*, Vol. 69, 1131–1135, 2020.
5. Wang, W., C. Chen, S. Wang, and W. Wu, "Switchable dual-band dual-sense circularly polarized patch antenna implemented by dual-band phase shifter of $\pm 90^\circ$," *IEEE Transactions on Antennas and Propagation*, Vol. 69, 6912–6917, 2021.
6. Liu, Y., Z. Yue, Y. Jia, Y. Xu, and Q. Xue, "Dual-band dual-circularly polarized antenna array with printed ridge gap waveguide," *IEEE Transactions on Antennas and Propagation*, Vol. 69, 5118–5123, 2021.

7. Ahmed, M. F., A. H. Shaalan, and K. H. Awadalla, "Design and simulation of a single fed multi-band circularly polarized microstrip antenna with slots," *Progress In Electromagnetics Research C*, Vol. 57, 71–79, 2015.
8. Zhang, L. and T. Dong, "RCS reduction using a miniaturized uni-planar electromagnetic band gap structure for circularly polarized microstrip antenna array," *Progress In Electromagnetics Research Letters*, Vol. 66, 135–141, 2017.
9. Zhu, J., Y. Yang, S. Li, S. Liao, and Q. Xue, "Dual-band dual circularly polarized antenna array using FSS-integrated polarization rotation AMC ground for vehicle satellite communications," *IEEE Transactions on Vehicular Technology*, Vol. 68, 10742–10751, 2019.
10. Ge, L., S. Gao, Y. Li, W. Qin, and J. Wang, "A low-profile dual-band antenna with different polarization and radiation properties over two bands for vehicular communications," *IEEE Transactions on Vehicular Technology*, Vol. 68, 1004–1008, 2019.
11. Li, Y., B. Tian, J. Xue, and G. Ge, "Compact dual-band circularly polarized antenna design for navigation terminals," *IEEE Antennas and Wireless Propagation Letters*, Vol. 15, 802–805, 2016.
12. Liang, Z. X., D. C. Yang, X. C. Wei, and E. P. Li, "Dual-band dual circularly polarized microstrip antenna with two eccentric rings and an arc-shaped conducting strip," *IEEE Antennas and Wireless Propagation Letters*, Vol. 15, 834–837, 2016.
13. Mao, C., Z. H. Jiang, D. H. Werner, S. S. Gao, and W. Hong, "Compact self-diplexing dual-band dual-sense circularly polarized array antenna with closely spaced operating frequencies," *IEEE Transactions on Antennas and Propagation*, Vol. 67, 4617–4625, 2019.